17th World Conference on Earthquake Engineering, 17WCEE

Sendai, Japan - September 13th to 18th 2020

HYSTERETIC EFFECTS ON SINGLE-STORY SYSTEM INELASTIC RESPONSE CONSIDERING TORSION

H. Soleimankhani[1], G. A. MacRae[2], T. J. Sullivan[3]

[1] *PhD Candidate, University of Canterbury, hossein.soleimankhani@pg.canterbury.ac.nz*
[2] *Professor, Tongji University & Associate Professor, University of Canterbury, gregory.macrae@canterbury.ac.nz*
[3] *Professor, University of Canterbury, timothy.sullivan@canterbury.ac.nz*

Abstract

This study investigates the effects of different hysteretic characteristics on the seismic response of single story systems subject to impulse excitations as well as a suite of earthquake records. Hysteretic loops considered are elasto-plastic, bilinear, Takeda, SINA, and flag-shaped. All these hysteretic loops have the same initial lateral stiffness and strength. An energy approach is used to explain the response of the systems to different types of ground shaking. Initial analyses are conducted using regular systems with no torsional response. Whereas later analyses considers torsional irregularity.

It is shown that for the impulse-type records, structures with the same backbone curve had the same maximum response irrespective of their hysteretic behavior. The peak responses for systems under impulse-type ground motions occur in the first major cycle and are similar. The likelihood of further displacement in the negative direction due to longer duration ground shaking is characterized based on a free vibration analysis and energy considerations. Hysteretic models with low energy dissipation such as SINA and flag-shaped loops are shown to have a greater likelihood of higher absolute displacement response in the negative direction and smaller residual displacements compared to those with fatter hysteretic loops. The understanding of the response in terms of energy reconciles some differences in the ability of initial versus secant stiffness based methods to predict peak displacement demands with account for different ground motion characteristics.

For systems with torsional response under impulse-type records, the elastic energy stored in the out-of-plane elements is released causing greater displacement on the weak side of the system in the reverse direction. Therefore, unlike systems with just translational response the peak displacement of systems with different hysteretic models under impulse-type ground shakings is not always the same.

Keywords: Hysteretic Model; Inelastic Seismic Response; Torsional Behavior.

1. Introduction

Generally, structural damage is considered to be related to displacements of the structure. Therefore, development of methods for estimation of displacement demand has long been recognized as a crucial part of seismic design and assessment. Since most structures under seismic excitation are expected to experience inelastic deformation, simple methods that give an estimation of peak inelastic response of systems are of special interest [1].

The displacement demand on an inelastic system may be affected by the hysteretic characteristics of the structural elements [2]. However, the influence of different hysteretic behaviour is not accounted for in most building design codes including NZS 1170.5 [3]. Generally, there are two common displacement prediction approaches. The first, which is commonly used by design standards, uses just the elastic response spectrum and a period of vibration associated with the initial stiffness to compute displacement demands on structures [4]. The second is built on the secant stiffness concept, which considers the full hysteretic behavior of the system [5].

Initial stiffness based methods assume that the design inelastic displacement of the structure is equal to the displacement of its companion elastic system for medium to long period structures (Fig. 1(a)). This is known as the equal displacement assumption (EDA) [4]. For shorter period structures, the inelastic displacements are often larger than elastic displacements. The equal energy assumption (EEA) explains this as shown in Fig. 1(b). Methods based on this concept are included in some modern building standards such as NZS 1170.5 [6]. These methods do not consider the total hysteretic behaviour of the system. Therefore, for structures with low energy dissipation such as pinched hysteretic structures, the displacements may be underestimated. As a result, modification factors, such as the C_2 factor in Equation (3-15) of FEMA 356, have been proposed to represent the effects of pinched hysteresis shape [7].

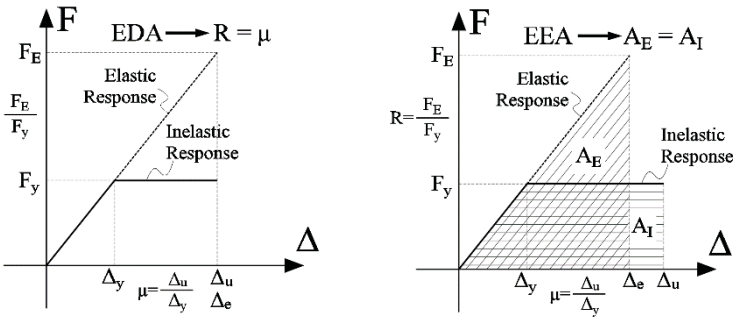

(a) (b)

Fig. 1– Illustration of the EDA and EEA.

The secant stiffness concept, introduced by Jacobsen [8] and followed by Gulkan et al. [5], is based on the concept that the energy absorbed by the hysteretic cyclic response of yielding structure in its steady state is equal to the energy dissipated by the equivalent viscous damping (EVD) of a structure with an elastic stiffness equal to the secant stiffness at the peak displacement. This method resulted in displacements close to those predicted by time-history analysis for structures with some hysteretic behaviour, such as the Takeda loop, but underestimated the displacement of systems with high energy dissipating capacity such as the bilinear model [9]. In order to improve the accuracy of this method, Priestley et al. [9] calibrated values of EVD for different hysteretic models based on the results of time-history analyses to predict the same peak displacement. By doing this, note that both approaches are empirical and the accuracy of their predictions will depend on the characteristics of the ground motions used in calibration studies compared to those expected at the site. Indeed, researchers such as Pennucci et al. [10] and Stafford et al. [11] showed that spectral shape and earthquake magnitude would affect calibration results.

From the discussion above, it would appear that the success of a given approach would greatly depend on the characteristics of the imposed shaking. To help address this, research has aims to identify modifications that can be made to address the limitations in the fundamental concepts of both methods. Furthermore, because floors in buildings subject to earthquake shaking both translate and rotate in plan (known as "building torsion"), the torsional response changes the shaking characteristics and may cause larger demands on one side of the building. Consequently, in order to design structures for earthquakes, there may be a need for inelastic displacement demand on buildings to be considered taking the effects of both hysteretic behaviour and torsion into account together.

2. Case study building

A numerical model of a single-story building is employed for analyses in this work. The results are used to explain the response of the oscillators with different hysteretic behaviour to impulse loading as well as ground shaking. The mass, M, and total initial stiffness, K_i, is set to result in a period of vibration, T, of one second ($K_i = (2\pi/T)^2 M$). The total lateral strength of the system, F_y, is set to have a yield strength ratio, C_y, of 0.1 (i.e. $F_y = C_y\,(M \times g)$ where g is the acceleration of gravity). The parameters defining the single-degree-of-freedom (SDOF) system are listed in Table 1.

Table 1 – Parameters to define the SDOF system

Parameter	Value	Unit
Mass (M)	4.00×10^6	N.s^2/m
Period (T)	1.00	s
Total Initial Stiffness (K_i)	1.58×10^8	N/m
Total Yield Strength (F_y)	4.00×10^6	N

In this study, "Torsionally Irregular" systems are those in which the center of mass, C_M, does not coincide with the centres of stiffness, C_R, and strength, C_V, and experience torsional response in addition to pure translation. Fig. 2 shows the plan view of a torsionally irregular building that is rectangular in plan with width, b, of 24 m and length, h, of 40 m. The total mass, M, and mass rotational inertia, I_{rot}, of the system are lumped at the center of mass. The system is eccentric in the Y direction and symmetric in the X direction. The eccentricity is due to larger stiffness and strength of the right hand side element. This building is shaken only in the North-South direction (the Y-direction) in this work.

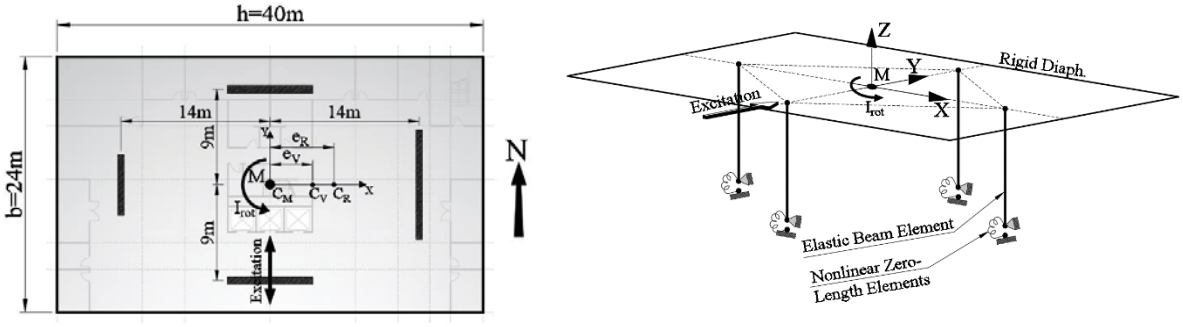

(a) (b)

Fig. 2 – (a) Plan view of the torsionally irregular case study building (b) Structural Model.

The stiffness, e_R, and strength, e_V, eccentricities are defined as the distances between C_M and C_R, and between C_M and C_V, respectively. Assuming that M is uniformly distributed over the plan, the I_{rot} of a rectangular plan can be simplified as $I_{rot} = M\,(b^2 + h^2) / 12$.

In addition to looking at pure translational response, the work will consider the single-story structure with strength/stiffness eccentricity to investigate the effect of hysteretic models on seismic response of torsionally irregular systems. The strength and its companion stiffness eccentricities are e_V = 0.1b and e_R = 0.15b respectively. The translational stiffness and strength of the system in both directions are assumed identical. The torsional stiffness of the building with the dimensions shown in Fig. 2 in term of its lateral stiffness is K_{rot} = 241 K_i (units: N and m). The parameters that define the torsionally irregular single-story system are listed in Table 2.

Table 2 – Parameters to define the torsionally irregular system

Parameter	Value	Unit
Strength Eccentricity (e_V)	4.00	m
Stiffness Eccentricity (e_R)	6.00	m
Mass Rotational Inertia (I_{rot})	7.25×10^{8}	N.s^2.m
Rotational Stiffness (K_{rot})	3.81×10^{10}	N.m

For systems under strong earthquake shaking, the force demand may exceed the system yield strength, F_y. From then on, the system unloading and reloading characteristics are needed in addition to its initial stiffness and damping to evaluate the seismic response of the system. Five different hysteretic models are employed in this study and are schematically described in Fig. 3.

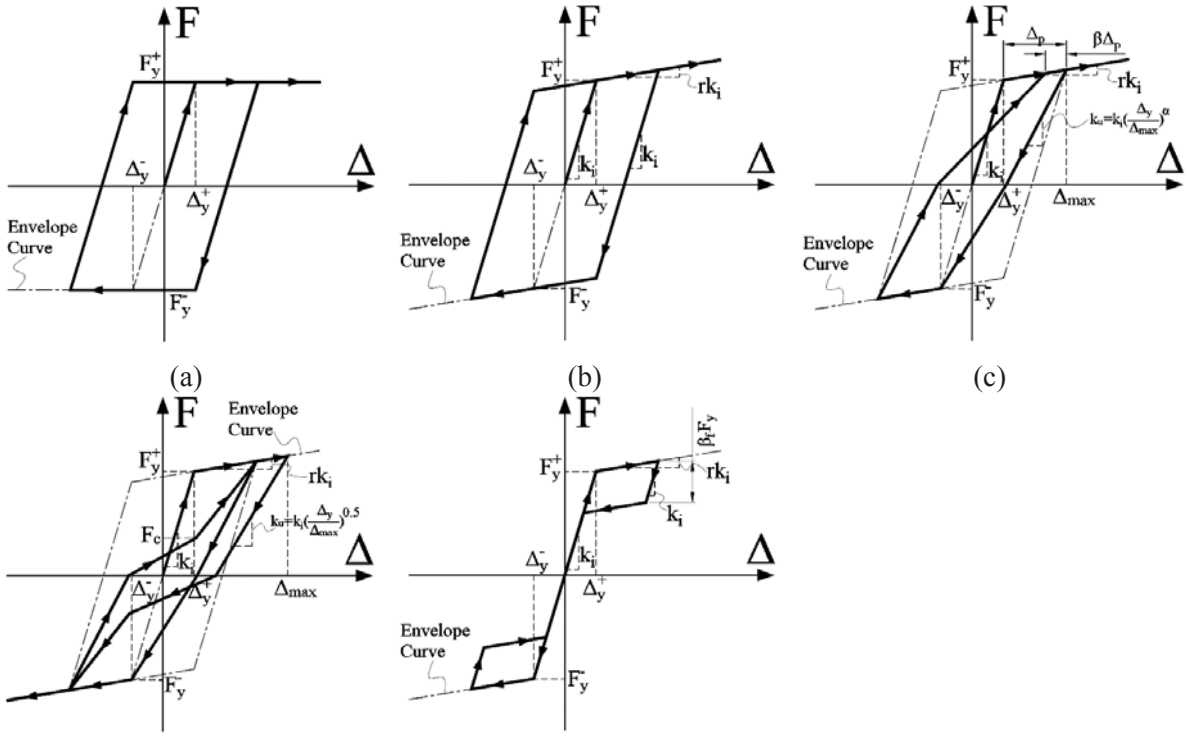

Fig. 3 – Hysteretic models (a) EPP (b) bilinear (c) Takeda (d) SINA (e) flag-shaped.

The first model is elastic-perfectly-plastic (EPP). It is characterized just by an initial stiffness, k_i, and yield strength, F_y. This model is the simplest model and assumes the same loading and unloading stiffness without incorporation of deterioration and or hardening. The EPP model has characteristics that represent some isolation systems and some structural systems with friction connections [12]. The second hysteretic model, called "bilinear", is similar to EPP except that strain hardening is incorporated

in this model. The post-yield stiffness ratio of $r = 0.05$ is assigned. The bilinear model with different values for r represents the cyclic behavior of steel structures and various base-isolated systems [9]. The Takeda model is commonly used to represent the behavior of reinforced concrete structures [13]. For this model, the α and β parameters define the unloading and reloading characteristics of the system. The SINA loop that suffers from significant stiffness deterioration is representative of pinched structural systems such as old reinforced concrete structures without proper ductile detailing [14]. The last hysteretic model, flag-shaped, with an unloading stiffness equal to the initial stiffness may represent some post-tensioned or self-centering systems. During unloading, after the lateral force decreases by $\beta_f F_y$ the displacement reduces to that from the initial elastic curve following the post-elastic slope.

Table 3 – Hysteretic parameters

Hysteretic Model	Parameters
Elastic-Perfectly-Plastic	k_i, F_y,
Bilinear	k_i, F_y, $r = 0.05$
Takeda (Thin)	k_i, F_y, $r = 0.05$, $\alpha = 0.5$, $\beta = 0.$
SINA	k_i, F_y, $r = 0.05$, $F_c = 0.3F_y$
Flag-Shaped	k_i, F_y, $r = 0.05$, $\beta_f = 0.5$

For the first part of the study, an impulse load is applied to the structure. The impulse load is $I = 1.73\times10^6$ N.s which causes a velocity, V, of 0.434 m/s. Three ground motions selected for time-history analyses are shown in Fig. 4.

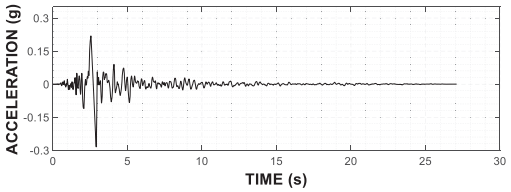

(a) 1979 Coyote Lake, Gilroy Array Station 6 – component 230

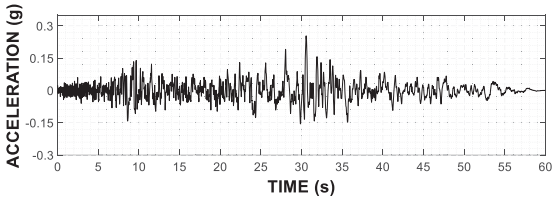

(b) 1992 Landers, Indio-Coachella Canal - component 90

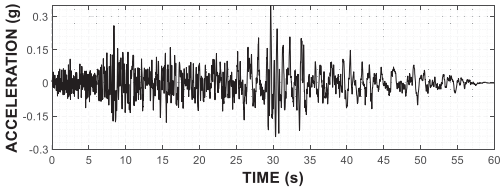

(c) 1992 Landers, Indio-Coachella Canal - component 00

Fig. 4 – Ground motions used for time-history analyses.

The first one, 1979 Coyote Lake earthquake recorded at the Gilroy Array Station 6, is representative of a short-duration ground shaking with a strong pulse impulse (Fig. 4(a)). The 5-75% significant duration, D_{S575}, of this ground motion is less than 0.9 s [15]. The next two ground motions are two components of 1992 Landers earthquake recorded at Indio-Coachella Canal, California (Fig. 4(b) & (c)). They can be considered more as long-duration cyclic-type ground motions. The 5-75% significant duration, D_{S575}, of these ground motions are about 25 s. These three ground motions are picked from a suite of 20 ground motion pairs selected according to Generalised Conditional Intensity Measure approach proposed by Bradley [16] for the subsoil class C in Wellington, New Zealand.

OpenSees [17] is used to perform the nonlinear time-history analyses (NLTHA) using Newmark integration scheme with time steps of $d_t = 0.01$ s. The viscous damping of 5% for the translational mode of vibration is assigned and a tangent stiffness proportional model is used. The mass proportional damping coefficient is ignored to have a more realistic estimation of damping of the system as discussed by Priestley et al. [9]. Analyses are conducted using a small displacement analysis regime with mass and elements as shown in Fig. 2.

3. SDOF System Response Considerations

3.1. Oscillators under impulse loading

The monotonic loading curve for bilinear, Takeda, SINA, and flag-shaped loops have the same backbone curve. The EPP loop has the same initial stiffness and strength as others but no post-yield stiffness. Therefore, with the exception of the EPP loop, under the very first excursion to the same ductility demand the area under the force-displacement curve for all hysteretic models are the same and larger than that of EPP.

The kinetic energy imparted to the system by an impulse is $E = \frac{1}{2} M \times V^2 = 3.76 \times 10^5$ N.m. For the impulse loading, the monotonic loading energy of the system is equal to the input energy if the damping energy is ignored (i.e. $\xi = 0.$). This energy, which the system has to dissipate and/or store, is the area under the force-displacement curve above the horizontal axis. Therefore, hysteretic loops with the same backbone curves go to the same displacement as shown in Fig. 5. However, larger displacement in the initial direction may occur for the EPP loop than others as shown in Fig. 6. In the figures below, F and Δ are the lateral force and lateral displacement of the system respectively.

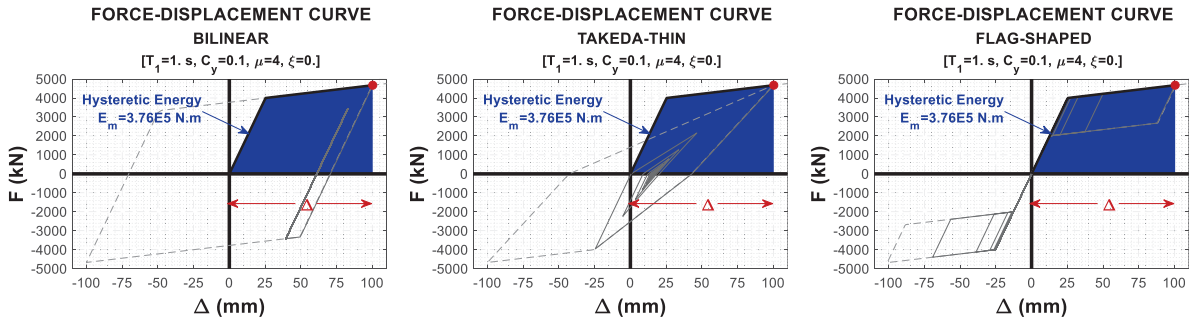

(a) (b) (c)

Fig. 5 – Response of SDOF system to impulse load (a) bilinear (b) Takeda-thin (c) flag-shaped, with hysteretic energy associated with initial impulse shown shaded.

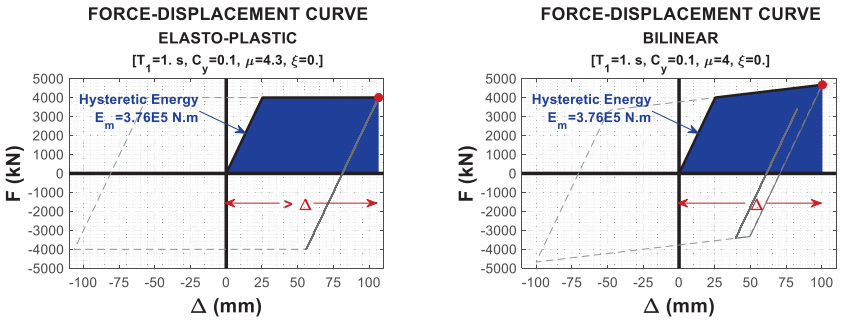

(a) (b)

Fig. 6 – Response of SDOF system to impulse load (a) EPP (b) bilinear, with hysteretic energy associated with initial impulse shown shaded.

3.2. Unloading behavior of the oscillators

The total absolute response of the system may also be affected by the unloading response, which causes displacement in the reverse (negative) direction. If damping is ignored and free vibration of the system is considered, the potential energy of the system pushes the system back towards the opposite direction. The larger this potential energy is, the more the system is pushed towards the original position.

The area above the horizontal axis and below the unloading path of the hysteretic loop at the peak displacement, where there is zero velocity, is the potential energy as shown by the blue area in Fig. 7. However, the area within the hysteretic loop is the dissipated energy shown by the green area [18].

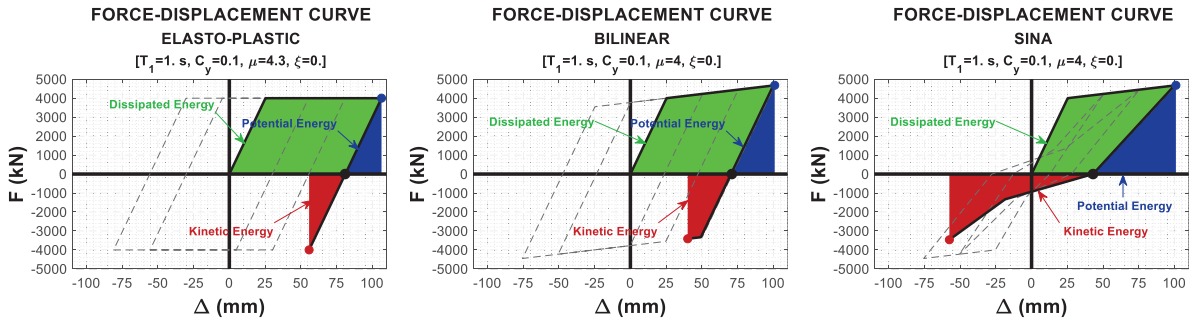

(a) (b) (c)

Fig. 7 – Unloading response of structure after loading to the same peak (a) EPP (b) bilinear (c) SINA. Areas of dissipated, potential and kinetic energy associated with a cycle of response are highlighted.

When the system is released from a peak displacement and moves back to zero force, the potential energy of the structure is converted into kinetic energy. At this point, the momentum puts the same amount of energy into the system towards the reverse direction as shown in the Fig. 7. The amount of potential energy and the displacement of the structure in the opposite direction are functions of unloading and reloading characteristics of the hysteretic model. It may be seen that the displacement towards the negative direction is larger for the SINA loop than for the bilinear and EPP loops. That can be explained as the SINA (as well as Takeda and flag-shaped) loop has less energy dissipation capacity and a greater amount of energy is stored in the monotonic direction compared to the bilinear and EPP loops. The larger the stored energy, the larger the potential to push the system in the reverse direction.

In all cases in Fig. 7, the peak displacement in the negative direction due to free vibration is less than that in the positive direction. For many structural systems used in practice, even when considering further earthquake shaking, the peak displacement in the negative direction may not exceed that in the positive direction. Therefore, in terms of maximum displacement, the response of the structures with different unloading characteristics can be expected to be the same for impulse-type loading. This is consistent with the EDA, which indicates that the structure peak displacements are only dependent on hysteresis curve's initial loading characteristics.

3.3. Illustrating the response of SDOF systems to impulse-type shaking

The SDOF system with different hysteretic models are subjected to the 1979 Coyote Lake – Gilroy Array #6 (Fig. 4(a)), with a strong pulse characteristic. The period of the ground motion pulse has been estimated to be 0.26 second. Fig. 8 shows that the maximum displacement of the system obtained from NLTHAs. Since the response follows the initial backbone curve, the maximum displacement is the same for all hysteresis loops, irrespective of the unloading characteristics as shown in Fig. 8(b) and (c). Since it never moves to the same absolute maximum displacement again in either direction, then the peak displacement is in the primary displacement direction. For loops with lower energy requirement to obtain the same displacement in the negative direction, these would have greater negative displacements when subject to the same motion as shown in Fig. 8(a) and (b).

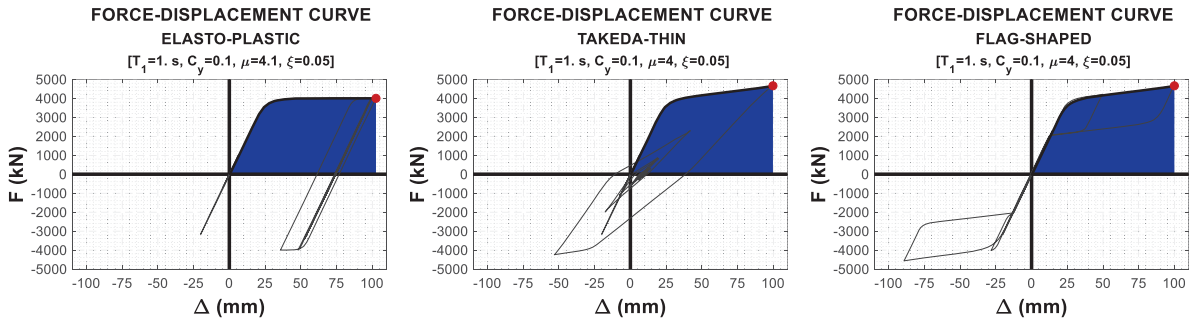

(a) (b) (c)

Fig. 8 – Response obtained from NLTHAs of a SDOF system subject to the 1979 Coyote Lake, Gilroy Array Station 6 – component 230 (a) EPP (b) Takeda (c) flag-shaped.

3.4. Illustrating the response of SDOF systems to longer duration earthquake shaking

For the same structures examined in Section 3.3 but subject to the 1992 Landers, Indio-Coachella Canal – component 90 (Fig. 4(b)), which is a relatively long-duration ground shaking record, the responses are given in Fig. 9. The results shows that peak displacements of structures with bilinear, Takeda, SINA, and flag-shaped loops increase as the energy dissipation capacity, given by the area within one stabilized full cycle, decreases. This increase in displacement is consistent with the demands predicted by the area-based EVD method. The exception to this is the EPP structure response, where the recentering tendency of such loops is lower and cumulative displacements in one direction can cause an increase in response [19].

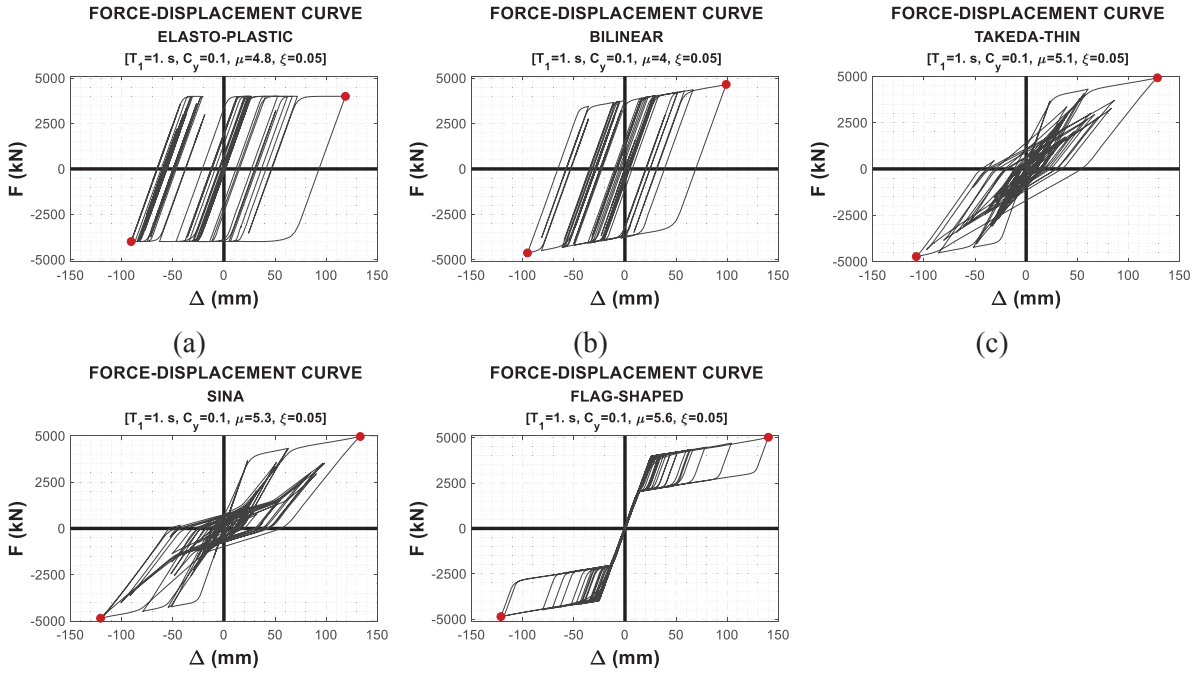

(a) (b) (c)

(d) (e)

Fig. 9 – Response of structure to 1992 Landers, Indio-Coachella Canal – component 90 (a) EPP (b) bilinear (c) Takeda (d) SINA (e) flag-shaped.

For structures without a strong dynamic recentering tendency, the likelihood of ratcheting is increased causing larger displacements [6]. This is particularly significant for hysteresis loops with low

- or negative - bilinear stiffness ratio [19]. This effect is more likely during long duration shaking [9]. This effect is consistent with the analyses undertaken here. The SDOF system is subjected to 1992 Landers, Indio-Coachella Canal – Component 00 shown in Fig. 4(c). Such ratcheting can easily be seen in Fig. 10(a) compared with Fig. 10(b) and (c). The peak displacement in the positive direction is much larger than that in the negative direction as the EPP model has no inherent tendency to go back towards the zero displacement position, which makes the displacement of this model accumulate in one direction. However, SINA and flag-shaped show larger recentering characteristics and oscillate about the zero displacement position. The recentering characteristics of loops such as SINA and flag-shaped tends more to push them back towards the center when they move away from their original position. This was explained by the potential energy concept in Section 3.2.

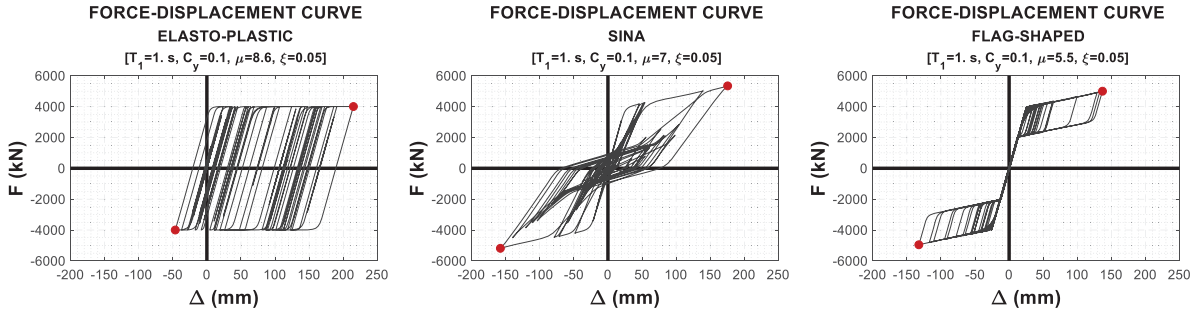

(a) (b) (c)

Fig. 10 – Ratcheting due to no post-yield stiffness subjected to 1992 Landers, Indio-Coachella Canal – component 00 (a) EPP (b) SINA (c) flag-shaped.

This effect is not considered explicitly in either the initial stiffness based or the area-based EVD methods. Therefore, both methods may be non-conservative for structures with negative post-elastic stiffness subjected to medium to long duration earthquakes [19]. Methods that have been calibrated to the results of NLTHAs, such as the calibrated EVD expressions in Pennucci et al. [20], will be more reliable but only if the ground motion characteristics used for calibration are similar to those expected at the site in question.

4. Torsional Consideration

The considerations above relate to structures where torsional effects are not significant. Systems with torsional irregularity under impulse-type ground shaking show similar trends to those without torsion. Torsionally regular and irregular systems with bilinear and SINA hysteresis loops have been subject to the 1979 Coyote Lake – Gilroy Array #6 record component 230 and results are shown in Fig. 11.

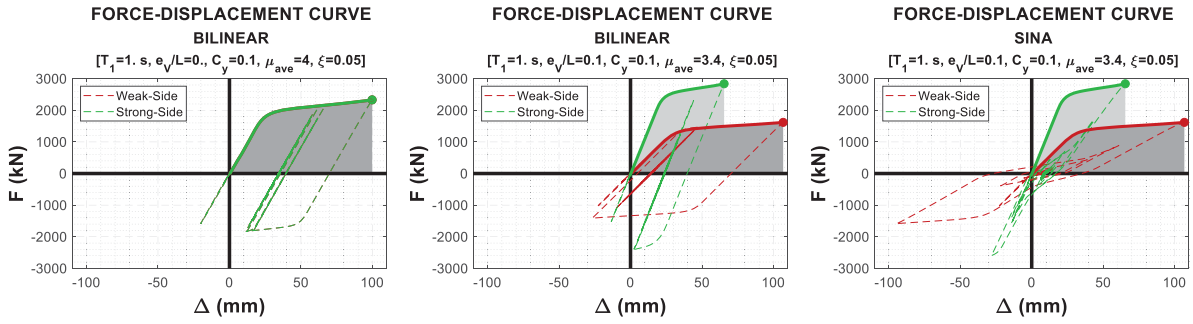

(a) (b) (c)

Fig. 11 – Response of a single-story torsionally irregular system to 1979 Coyote Lake, Gilroy Array Station 6 – component 230 with different hysteretic characteristics: (a) bilinear – e_V=0 (b) bilinear – e_V≠0 (c) SINA - e_V≠0.

As can be seen in Fig. 11(b) and (c), the system maximum displacement demand is the same for both systems because the peak displacement in elements on both the weak and strong sides of the structure occurs under the first major impulse following the initial backbone curve. Since this ground motion was not strong enough after the pulse, the structural elements did not reach the peak displacement again and the difference in unloading stiffness plays no role in terms of the maximum system demand.

However, for the torsionally irregular systems, the elements perpendicular to the direction of loading also absorb energy as the building twists. The energy taken by the out-of-plane elements reduces the energy input into elements in the direction of loading and this in turn reduces the average in-plane system displacement compared to that of systems without torsional irregularity (Fig. 11(a), (b)). This could be one contributing reason to explain why displacement of center of mass usually decreases slightly as the strength (and/or stiffness) eccentricity of the system increases.

When a torsionally irregular structure with elements in the perpendicular direction (providing torsional restraint) is pushed to a certain displacement, the recoverable strain energy stored in the system increases compared to a system without any torsion. It may cause the element with the largest displacement in the direction of loading to undergo increased displacement in the reverse (negative) direction. This was seen in Fig. 11(c) for the pinched loop compared to Fig. 11(b). In addition, as can be seen in Fig. 12, for the weaker element of the system (the red line), the ratio of the displacement in the negative direction to that in the positive direction is larger for the case of the torsionally irregular system (Fig. 12(b)) than for the torsionally regular system (Fig. 12(a)). That is because the energy stored in out-of-plane elements was used by the weaker element making it displace more in the negative direction.

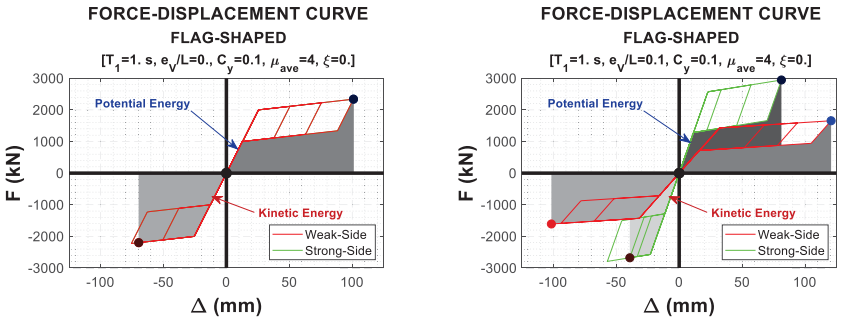

(a) (b)

Fig. 12 – Unloading response of system with and without torsional irregularity after loading to the peak (a) torsionally regular (b) torsionally irregular.

Fig. 13(a) shows the system without eccentricity under the impulse-type 1979 Coyote Lake – Gilroy Array #6 record. As discussed before, the system without eccentricity responds to the peak displacement under the first major impulse following its initial backbone curve and then it is less likely to get to an absolute displacement larger than the first peak.

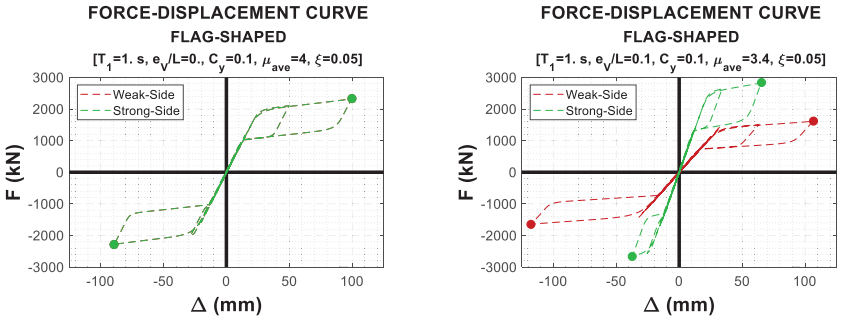

(a) (b)

Fig. 13 – Response of Single-Story System to 1979 Coyote Lake, Gilroy Array Station 6 – Component 230 (Impulse-type GM) (a) torsionally regular (b) torsionally irregular.

Under the first major impulse, both the weak and strong sides of the structure move to the peak displacement in the primary direction (Fig. 13(b)). When the system reaches the peak displacement in the primary direction, the extra energy imparted by the ground shaking along with the energy stored in the whole system are mainly mobilized to displace the weaker element in the reverse direction beyond its peak displacement in the positive direction. Therefore, for torsionally irregular systems, even under a ground shaking with just one strong pulse, the peak response is dependent on the hysteretic model even though it was shown in Section 3.3 that for regular systems it is often independent of the unloading properties of the loop.

5. Conclusions

The response of single-story structures with different hysteretic models under impulse-type and long duration earthquake ground shaking has been examined. Five different hysteretic models are considered in this study and effects of hysteretic behavior on seismic response of the system is explained using energy considerations. Analyses of systems with torsional response have also been carried out to explore the effects of hysteretic behavior and ground motion characteristics on torsional response.

For structural systems with the same backbone curve subject to earthquake records, the response depended on both the shaking duration and the hysteresis loop shape. Short duration records, which acted like impulse records, gave the same peak displacement for oscillators with the same loading characteristics irrespective of the unloading characteristics. However, for long duration records, a significant number of oscillations occurred, but this was more significant for hysteresis loops with low resistance to oscillations, such as pinched loops.

For torsionally irregular systems subject to impulse records, the peak displacement does not necessarily occur during the major pulse. For hysteretic models with large energy dissipation capacity, the peak displacement may be simply a function of backbone curve. However, for systems with small energy dissipation (e.g. flag-shaped with small flag size) the peak value depends on the full hysteretic behavior of the system. The energy stored in the out-of-plane elements releases in the unloading phase of the response and along with the energy imparted by the ground shaking can cause the weaker element of the system to have larger displacement in the reverse direction. This indicates that considerations in the secondary direction are important to consider for torsion as well as for normal torsionally restrained structure displacement prediction.

6. References

[1] E. Miranda, "Estimation of Inelastic Deformation Demands of SDOF Systems," *Journal of Structural Engineering,* vol. 127, no. 9, pp. 1005-1012, 2001.

[2] M. J. N. Priestley, "Displacement-Based Seismic Assessment of Reinforced Concrete Buildings," *Journal of Earthquake Engineering,* vol. 1, no. 1, pp. 157-192, 1997.

[3] H. Judi, R. C. Fenwick and B. J. Davidson, "Influence of hysteretic form on seismic beahviour of structures," in *NZSEE*, 2002.

[4] S. Veletsos and N. Newmark, "Effect of Inelastic Behavior on the Response of Simple Systems to Earthquake Motions," Japan, 1960.

[5] P. Gulkan and M. Sozen, "Inelastic Responses of Reinforced Concrete Structures to Earthquake Motions," *ACI Journal,* vol. 71, no. 12, pp. 604-610, 1974.

[6] NZS1170.5:2004, "Structural Design Actions - Part 5: Earthquake actions - New Zealand Incorporating Amendment No. 1," Standards New Zealand, Wellington, New Zealand, 2016.

[7] FEMA 356, "Prestandard and Commentary for the Seismic Rehabilitation of Buildings," prepared by ASCE for the Federal Emergency Management Agency, Washington, D.C., 2000.

[8] L. Jacobsen, "Damping in Composite Structures," Tokyo, Japan, 1960.

[9] M. J. N. Priestley, G. M. Calvi and M. Kowalsky, Displacement-Based Seismic Design of Structures, Pavia, Italy: IUSS PRESS, 2007.

[10] D. Pennucci, T. J. Sullivan and G. M. Calvi, "Displacement Reduction Factors for the Design of Medium and Long Period Structures," *Journal of Earthquake Engineering,* vol. 15, no. S1, pp. 1-29, 2011.

[11] P. J. Stafford, T. J. Sullivan and D. Pennucci, "Empirical Correlation between Inelastic and Elastic Spectral Displacement Demands," *Earthquake Spectra,* vol. 32, no. 3, pp. 1419-1448, 2016.

[12] M. Hatami, G. MacRae, G. Rodgers and C. Clifton, "Numerical and Experimental Study on Friction Connections Performance - Asymmetric and Symmetric (AFC/SFC)," Auckland, New Zealand, 2019.

[13] T. Takeda, M. Sozen and N. Nielsen, "Reinforced Concrete Response to Simulated EarthQuakes," *Journal of Structural Divisions,* pp. 19-26, 1971.

[14] M. Saiidi and M. Sozen, "Simple and Complex Models for the Nonlinear Seismic Response of Reinforced Concrete Structures," Department of Civil Engineering, University of Illinois, Urbana, Illinois, USA, 1979.

[15] S. Kramer, Geotechnical Earthquake Engneering, New Jersey: Prentice Hall, 1996.

[16] B. A. Bradley, "A Generalised Conditional Intensity Measure Approach and Holistic Ground Motion Selection," vol. 39, no. 12, 2010.

[17] F. McKenna and G. Fenves, "Open System for Earthquake Engineering Simulation," University of California: Berkely, California, 2000.

[18] A. Chopra, Dynamics of Structures, Englewood Cliffs, New Jersey: Prentice-Hall, 1995.

[19] G. A. MacRae, "P-Δ Effects on Single-Degree-of-Freedom Structures in Earthquakes," *Earthquake Spectra,* vol. 10, no. 3, pp. 539-568, 1994.

[20] D. Pennucci, G. M. Calvi and T. J. Sullivan, "Displacement-Based Design of Precast Walls with Additional Dampers," *Journal of Earthquake Engineering,* vol. 13, no. S1, pp. 40-65, 2009.

